May 2016

Multi-Scale Modeling of Particle Reinforced Concrete Through Finite Element Analysis

Mir Zunaid Shams
University of Wisconsin-Milwaukee

MULTI-SCALE MODELING OF PARTICLE REINFORCED CONCRETE THROUGH FINITE ELEMENT ANALYSIS

by

Mir Zunaid Shams

A Thesis Submitted in

Partial Fulfillment of the

Requirements for the Degree of

Master of Science

in Engineering

at

The University of Wisconsin-Milwaukee

May 2016

ABSTRACT

MULTI-SCALE MODELING OF PARTICLE REINFORCED CONCRETE THROUGH FINITE ELEMENT ANALYSIS

by

Mir Zunaid Shams

The University of Wisconsin-Milwaukee, 2016
Under the Supervision of Professor Konstantin Sobolev

Concrete is the main constituent material in many structures. The behavior of concrete is nonlinear and complex. Increasing use of computer based methods for designing and simulation have also increased the urge for the exact solution of the problems. This leads to difficulties in simulation and modeling of concrete structures. A good approach is to use the general purpose finite element software, e.g ANSYS . Normal strength concrete is a composite material represented by mechanically strong aggregates of various shapes and sizes incorporated into weaker cementitious matrix. A number of simplified homogenized models have been reported in the literature to represent the mechanical response of concrete. An accurate representation of the spatial distribution of the aggregate particles is one of the most important aspects of real-scale concrete modeling. A three-dimensional, numerical model, capable of predicting structural reliability of concrete under various loading conditions has been developed. A micromechanical heterogeneous model based on "real world" spatial distribution of aggregates was generated using a packing algorithm. This model has been used to compute the stress-strain response of

concrete by taking a representative cell homogenization approach. The results of numerical analysis of this model were compared with existing models of particulate composite material. The computational results demonstrate agreement within existing models and, therefore, can be used for micromechanical modeling of composite material such as "real world" concrete composites.

TABLE OF CONTENTS

LIST OF FIGURES

LIST OF TABLES

ACKNOWLEDGEMENTS

I would like to first and foremost thank my advisor, Dr. Konstantin Sobolev, for his continuous support and guidance. He has been generously patient with me and my constant questions.

I would like to express my gratitude to Dr. Ilya Avdeev for his valuable advices in several stages in this research. It was a pleasure working with Reza Moini and Scott Muzenski. Their contribution was vital for completing this thesis. I am grateful to Mehdi Gilaki who helped me in Finite Element Modeling. It would be very difficult to complete this thesis on time without his help.

I would like to appreciate all the help from Betty Warras at CEAS and Jenna Jazna at the Graduate School.

Finally, I would like to thank my family for being so supportive and for being a ceaseless inspiration to me.

CHAPTER 1

1 Introduction

The macro-mechanical material properties and behavior of portland cement and asphalt concrete mixtures, such as mechanical strength, modulus of elasticity, creep parameters, and shrinkage, greatly depend on the properties of their main constituent, the aggregates [1]. In addition to material properties, the most important parameters affecting the macro-mechanical behavior of particulate composite materials include packing density, compaction degree, particle size, and spatial distribution of aggregates. It has been shown that aggregates packing methods and optimal aggregate distribution can improve the mechanical response of concrete [1, 2].

Figure 1 depicts five classical models describing the micro-mechanical properties of composites applicable to concrete. The closed form expressions that are derived from these models for the homogenized modulus of elasticity (E_c) are summarized as follows [4, 6].

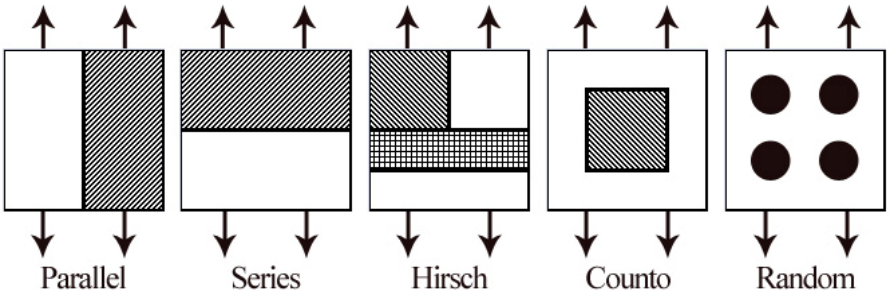

Figure 1-1: Various simplified matrix/aggregate models for macro-mechanical behavior [4, 6].

Parallel [4]
$$E_c = E_p V_p + E_m V_m \quad (1)$$

Series [4]
$$\frac{1}{E_c} = \frac{V_p}{E_p} + \frac{V_m}{E_m} \quad (2)$$

Hirsch [4]

$$\frac{1}{E_c} = X\left(\frac{1}{E_p V_p + E_m V_m}\right) + (1-X)\left(\frac{V_p}{E_p} + \frac{V_m}{E_m}\right) \quad (3)$$

Counto [4]

$$\frac{1}{E_c} = \frac{1-V_p^{\frac{1}{2}}}{E_m} + \frac{1}{\left(\frac{1-V_p^{\frac{1}{2}}}{V_p^{\frac{1}{2}}}\right)E_m + E_p} \quad (4)$$

Random (Maxwell Model) [6]

$$E_c = E_m\left[\frac{1+2V_p\left(\frac{E_p}{E_m}-1\right)\Big/\left(\frac{E_p}{E_m}+2\right)}{1-V_p\left(\frac{E_p}{E_m}-1\right)\Big/\left(\frac{E_p}{E_m}+2\right)}\right] \quad (5)$$

In the equations (1) – (5), V_p is the volumetric proportion of particulate, E_p is the elastic modulus of the particulate, V_m is the volumetric proportion of the matrix, and E_m is the elastic modulus of the matrix.

1.1 Motivation and Objectives

Engineered structures must be capable of performing their functions throughout a specified lifetime while being exposed to a series of events that include loading, environment, and damage threats. These events, either individually or in combination, can cause structural degradation, which, in turn, can affect the ability of the structure to perform its function. The performance degradation in structures made of composites is quite different when compared to metallic components because the failure is not uniquely defined in composite materials. The size of the material components is significantly smaller than the structural dimensions. The nonlinear behavior of concrete can be attributed to the initiation, propagation, accumulation and coalescence

of micro cracks within the internal material structure. Thus, failure of concrete structures is a multi-scale phenomena.

Since the beginning of the 1970s there has been a steadily increasing interest in developing robust and reliable models that can simulate concrete cracking; much of the development is certainly caused by the introduction of the finite element method and other numerical simulation techniques in science and engineering.

Improvements in the computer models may eventually reduce the role of experiments. Experiments are considered expensive, time consuming and cumbersome, only limited structural conditions can be tested, some loading situations are so complex that testing is considered impossible.

In this research, a Finite Element (FE) model was developed to analyze particle reinforced concrete. A prior FE model of a solid non-reinforced concrete was used as a benchmark.

1.2 Literature Review

In a research article Nagai et. al. demonstrated a method of finite element mesh generation in aggregate packed concrete. They pointed out that the difficulty in mesh generation comes from the boundary of aggregate and mortar. They proposed a method where they used three-dimensional digital image processing to generate mesh. They reported that they have developed the algorithm of a new element for the aggregate-mortar interface zone [7].

A finite element simulation using ANSYS based on a test for compressive strength of recycled coarse aggregate-filled concrete was presented by Jing et. al. in a research article

published in the Advanced Materials Research Journal. Opened crack and closed crack were introduced through transfer coefficient in their finite element model [8]. However, the meshing technique with the presence of aggregates in the specimen was not reported. Discussion about handling the aggregate and mortar interface zone was also not available.

The method of generation of aggregates in a computational model is very important to replicated the real world concrete. Leite et al. described a method of aggregate distribution with the help of random number generation [9]. Their objective was to develop a mesocopic concrete for simulating fracture processes.

He et. al. investigated the influence of aggregate packing on the elastic properties of concrete [10]. They developed a numerical model where they packed triangular aggregates. In a 2D finite element model, each triangular aggregate particle had a corresponding circular aggregate. Increase and decrease of Young's Modulus and Poisson's Ratio based on the change of area fraction of aggregates were reported.

Use of lattice model for computational model of concrete is also found to be used by several researchers [11]. Elias and Stang developed a 2D lattice model to demonstrate concrete aggregate interlocking. The model is based on rigid cells interconnected by springs.

Gal and Kryvoruk demonstrated a two step homogenization method of fiber reinforced concrete for multi-scale analysis [12]. Their homogenization approach includes first an analytical method to homogenize the aggregates and their interfacial zones and then a numerical homogenization algorithm is applied to homogenize the mortar, fibers and pre-homogenized aggregates. In another research Wriggers and Moftah developed a finite element model of concrete by incorporating aggregates, which were randomly generated using Monte Carlo's simulation

method [13]. Their meso-scale model was meshed using aligned approach for direct computation of the concrete effective properties. They have reported a subsequent homogenization was required during the numerical simulation.

Due to the highly non-homogenous nature of concrete it is necessary to analyze a concrete model in multi-scale to fully understand the role of every component, such as, aggregates, voids, reinforcing fibers etc. In his doctoral thesis, Kasai presented his work on multi-scale modeling of concrete in a nano-scale [14]. The author found a difference of themechanical properties of solid C-S-H between MD computation results and the nanoindentation-micromechanics combined results. His explanation was that may be due tothe difference of the real structure of C-S-H and the crystal structure of jennite andtobermorite . In another multi-scale approach, Choudhuri utilized XEFG-method to analyze concrete material both on macroscopic and mesoscopic scale [15]. Constituents of concrete, i.e. cement paste and aggregates, are modeled explicitly while concrete is consideredas homogenized material on the macrscopic scale. Purpose of the research was to represent concrete damage. non-linear isotropic damage model is used to describe the tensile behavior of the cement paste. A cohesive crack model is introduced that can capture complex mixed-mode fracture.

CHAPTER 2

2 Concrete Failures and Fracture

Concrete used in common engineering structures, basically is a composite material, produced using cement, aggregate and water. Sometimes, as per need some chemicals and mineral admixtures are also added. Experimental tests show that concrete behaves in a highly nonlinear manner in uniaxial compression. Figure.1 shows a typical stress-strain relationship subjected to uniaxial compression. This stress-strain curve is linearly elastic up to 30% of the maximum compressive strength. Above this point tie curve increases gradually up to about 70-90% of the maximum compressive strength. Eventually it reaches the pick value which is the maximum compressive strength. Immediately after the pick value, this stress-strain curve descends. This part of the curve is termed as softening. After the curve descends, crushing failure occurs at an ultimate strain. A numerical expression has been developed by Hognestad [16], which treats the ascending part as parabola and descending part as a straight line. This numerical expression is given as:

$$0 < \varepsilon < \varepsilon_0', \qquad \frac{\sigma}{\sigma_{cu}} = 2\frac{\varepsilon}{\varepsilon_0'}\left(1 - \frac{\varepsilon}{2\varepsilon_0'}\right)$$

$$\varepsilon_0' < \varepsilon < \varepsilon_{cu}, \qquad \frac{\sigma}{\sigma_{cu}} = 1 - 0.15\left(\frac{\varepsilon - \varepsilon_0'}{\varepsilon_{cu} - \varepsilon_0'}\right)$$

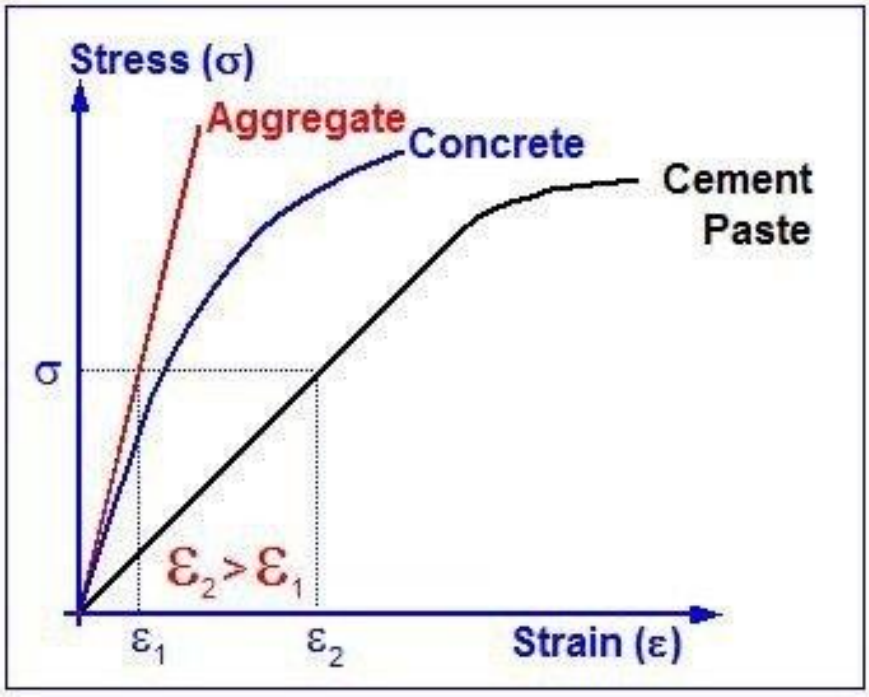

Figure 2.1 Typical Stress-strain curve for concrete and its constituents [9]

The stress-strain curve for hardened cement paste is almost linear as shown in the figure. The aggregate is more rigid than the cement paste and will therefore deform less (i.e. have a lower strain) under the same applied stress. The stress strain curve of concrete lies between those of the aggregate and the cement paste. However this relationship is non-linear over the most of the range. The reason for this non-linear behavior is that micro-cracks are formed both at the interface between aggregate particles and cement paste and within the cement paste itself.

Concrete taken through a cycle of loading and unloading will exhibit a stress-strain curve as shown in the Figure 2.2. Concrete will not return to its original length when unloading mainly due to creep and micro-crackling.

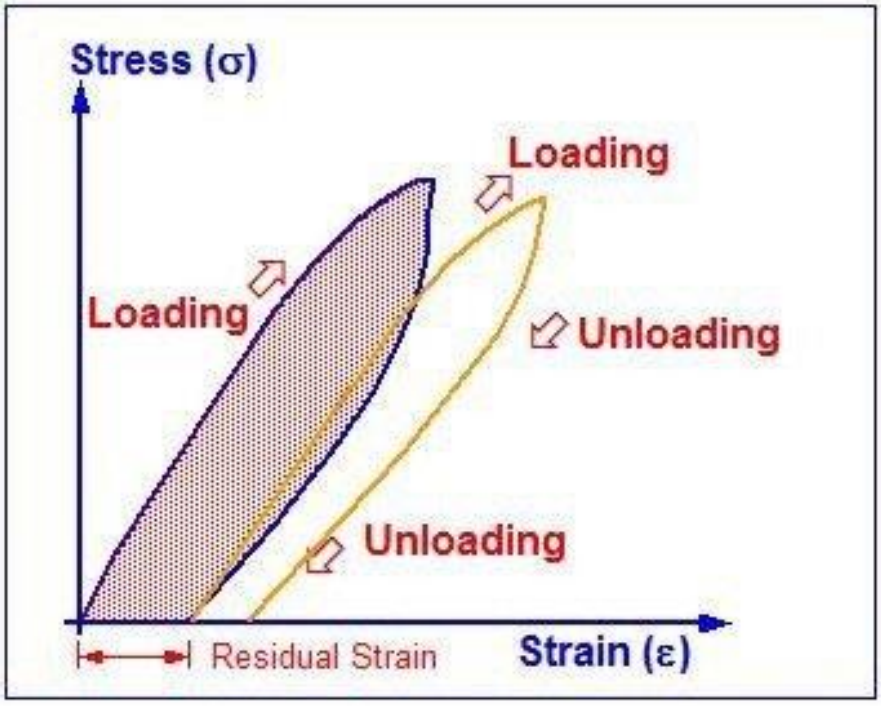

Figure 2.2 Loading and unloading cycle of concrete [9]

2.1 Multi-scale Modeling Basics

Many scientific and engineering problems involve multiple scales, particularly multiple spatial or temporal scales or both. Spatial scale involves the physical size of the problem and temporal scale involves the different constituents such as, composite materials, porous media etc. Involvement either spatial or temporal scale increases the complexity of the problem by increasing the size of computation. These types of problems can be efficiently handled by multi-scale modeling. In most traditional multi-scale modeling the calculation of material properties or system behavior on the macroscopic level is done using information or models from microscopic levels. In other words it captures the small scale effect on the large scale, without resolving the small-

scale features. At present there is enormous interest in multi-scale approaches, where the behavior of materials and structures is analyzed simultaneously at several different length-scales. The global mechanical performance of materials is determined by the materials structures and the local properties of constituents. The constituents also have their own material structures at a lower scale, which determine their mechanical properties. Take cement-based materials as an example. Concrete is a composite material consisting of coarse aggregates and mortar. The global mechanical behavior of concrete is determined by the material structure of concrete and the mechanical properties of coarse aggregates and mortar. At a lower scale mortar is made up with sands in cement paste. The properties of mortar are related to the material structure of mortar, as well as the local properties of sands and cement paste.

Homogenization method [17] and concurrent method [18] are usually employed to address the failure modeling problem of heterogeneous materials. The homogenization method applies when the scales can be ideally divided and separated, while the concurrent method is used when the scales are somehow coupled. Generally speaking the homogenization method consumes less computational resources, and the concurrent method provides more accurate simulation results.

The homogenization method requires that each block of heterogeneous material is taken out and isolated to evaluate its mechanical properties, and then these properties are used as the homogenized properties of the blocks and are put back to the network to simulate the global performance of the original piece of material. The concurrent method demands that the connection between neighboring blocks is preserved and the boundaries of blocks remain compatible with each other during the simulation, the stress and strain also remain the same as if the domain was not decomposed.

2.2 Multi-scale Finite Element Model (MsFEM)

Multi-scale Finite Element Model (MsFEM) typically works by capturing the multi-scale structure of the solution via localized basis functions. Basis functions contain information about the scales that are smaller than the local numerical. Basis functions are coupled through a global formulation to provide a faithful approximation of the solution. MsFEM consists of two major ingredients: multi-scale basis functions and global numerical formulation that couples these multi-scale basis functions. Basis functions are formulated to incorporate localized multi-scale features of the solution. A global formulation couples these basis functions to provide an accurate approximation of the solution.

Mathematical formulation of MsFEM can be developed by considering a linear elliptical equation as:

$L_u = f \quad in \ \Omega$ (2.1)

$u = 0 \quad on \ \partial\Omega$

Where Ω is a domain in $\mathbb{R}^d \qquad (d = 2,3)$

$$L_u = -div(k(x)\nabla u)$$

And $k(x)$ is a heterogeneous field varying over multiple scales.

It is additionally assumed that the tensor $k(x) = \left(k_{ij}(x)\right)$ is symmetric and satisfies

$\alpha|\xi|^2 \leq k_{ij}\xi_i\xi_j \leq \beta|\xi|^2$, for all $\xi \in \mathbb{R}^d$ and with $0<\alpha<\beta$

2.2.1 Construction of Basis Functions

The domain of interest is first decomposed into partitions called coarse grid and assume that the coarse grid can be resolved through a finer resolution called fine grid. Let us consider that T_h be a usual coarse grid partition of Ω into finite elements (triangular, quadrilaterals, etc.).

Let x_i be the interior nodes of T_h and φ_i^0 be the nodal basis of the standard finite element space $W_h = span\{\varphi_i^0\}$. For simplification, it is assumed that W_h consists of piecewise linear functions if T_h is a triangular partition. Definition of multi-scale basis function φ_i is given by:

$$L\varphi_i = 0 \text{ in } K,\ \varphi_i = \varphi_i^0 \text{ on } \partial K,\ \forall K \in T_h,\ \ K = S_i \qquad (2.2)$$

Where $S_i = supp\{\varphi_i^0\}$

These multi-scale basis functions coincide with standard finite element basis functions on the boundaries of a coarse-grid block *K*, and are oscillatory in the interior of each coarse-grid block. Computational domain smaller than coarse grid block *K* can be chosen if one can use smaller regions (K_{loc}) to characterize the local heterogeneities within the coarse-grid block. Such regions are called Representative Volume Elements (RVE). In this case the definition of multi-scale basis function φ_i changes to:

$$L\varphi_i = 0 \text{ in } K_{loc},\ \varphi_i = \varphi_i^0 \text{ on } \partial K_{loc},\ \forall K_{loc} \in T_h,\ \ K_{loc} = S_i \qquad (2.3)$$

In general, the equation (2.2) is solved on the fine grid to compute basis functions. In Figure 2.3a the basis function is consgtructed when K is a coarse partition element, and in Figure 2.3b the basis function is constructed by taking K to be an element smaller than the coarse grid block size.

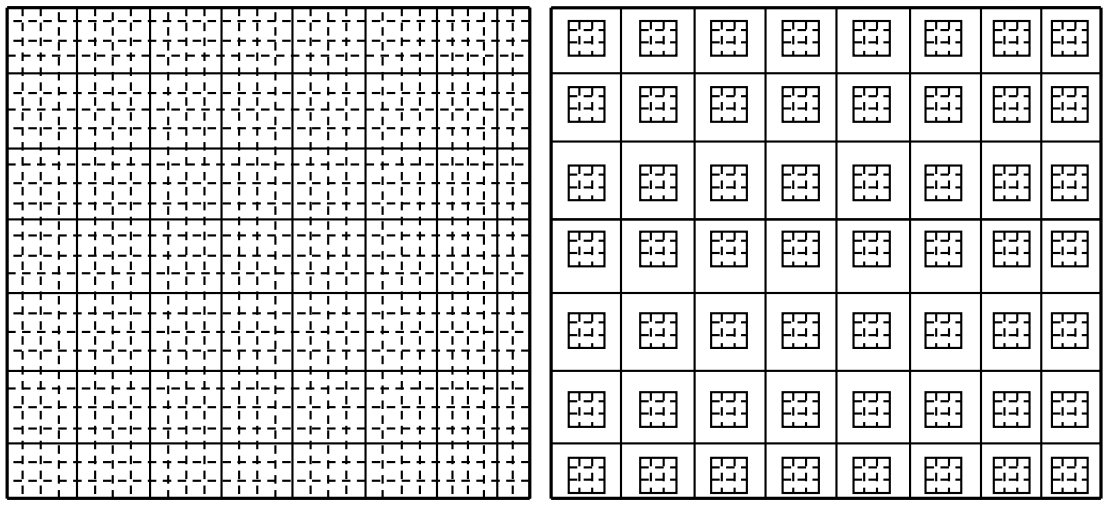

(a) (b)

Figure 2.3 Schematic descriptions of coarse and fine grids.

2.2.2 Global Formulation

The representation of the fine-scale solution through multi-scale basis functions allows reducing the dimension of the computation. Then the approximation of the solution $u_h = \sum_i u_i \varphi_i$ is substituted into the fine-scale equation. Here u_i are the approximate values of the solution at coarse grid nodal points. The resulting system is projected onto the coarse dimensional space to find u_i. This can be done by multiplying the resulting fine scale equation with coarse-scale test functions.

Generalized MsFEM problem is then represented as:

Find $u_h = V_h$ such that

$$\sum_K \int_K K \nabla u_h . \nabla v_h dx = \int_\Omega f v_h dx \qquad \forall v_h = V_h \tag{2.3}$$

The above equation (2.3) is equivalent to $Au_{nodal} = b$

Where $A=(a_{ij})$ with

$$a_{ij} = \sum_K \int_K k \nabla \varphi_i . \nabla \varphi_j dx$$

$U_{nodal} = (u_1, u_2, \ldots, u_i, \ldots)$ are the nodal values of the coarse scale solution and $b = (b_i)$ with

$$b_i = \int_\Omega f \varphi_i$$

Computation of a_{ij} requires the evaluation of the integrals using simple quadrature rule on the fine grid.

MsFEM can be further generalized as:

$$Lu = f \qquad (2.4)$$

Where $L: X \rightarrow Y$ is an operator.

Multi-scale basis functions are replaced by multi-scale maps $E^{MsFEM}: W_h \rightarrow V_h$

For each $v_h \in W_h$, $v_{r,h} = E^{MsFEM} v_h$ is defined as:

$L^{map} v_{r,h} = 0$ in K

L^{map} captures the small scales.

Solution scheme of equation (2.4) can be:

Find $u_{t,h} \in V_h$ such that: $\langle L^{gobal} u_{r,h}, v_{r,h} \rangle = \langle f, v_{r,h} \rangle, \qquad \forall v_{r,h} \in V_h$

Appropriate choises of L^{map} and L^{global} are the essential part of MsFEM and guarantee the convergence of the solution.

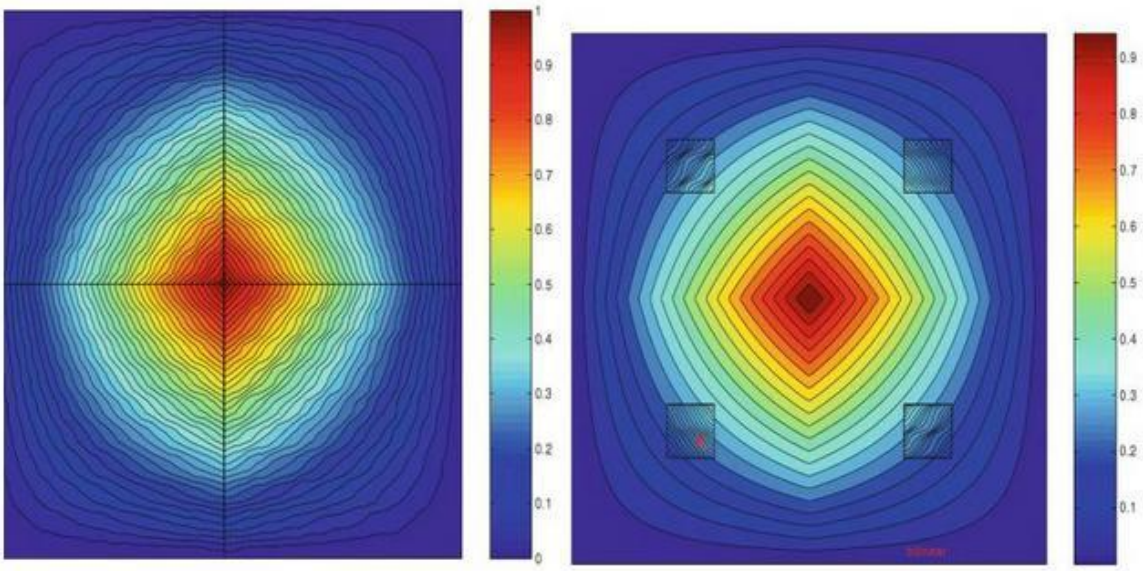

Figure 2.4 Basis functions example. Left: basis function with K being a coarse element. Right: basis function with K being RVE. [12]

CHAPTER 3

3 Computational Models

Most engineering problems are solved using mathematical/numerical modeling. Mathematical models are presented in terms of differential equations with a set of boundary and/or initial conditions. Figure 3-1 shows a flow chart of engineering problem solving process.

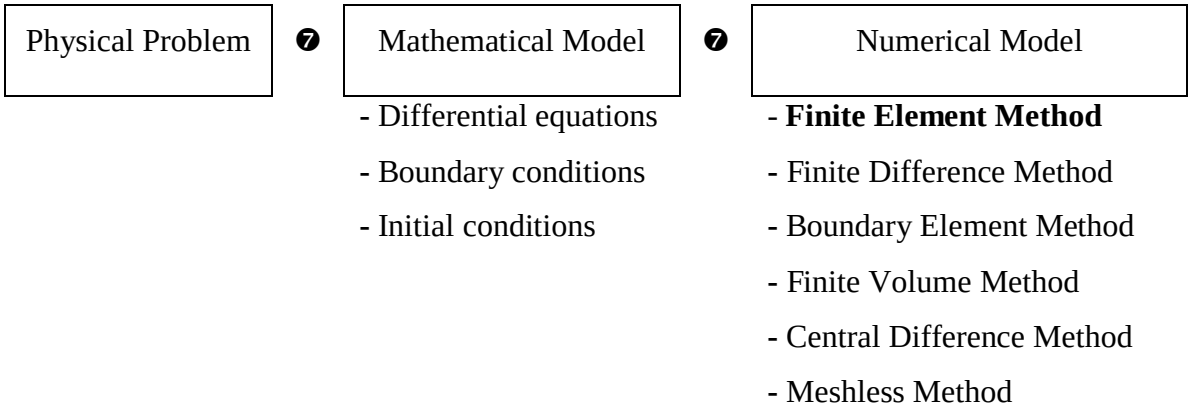

Figure 3-1: Engineering problem solving process

Numerical models approximate exact solutions at discrete points of a given physical system. FEA is a popular numerical technique to solve engineering problems because of its ability to handle complex structures.

3.1. The Packing Algorithm

Given the relationship between input parameters and output material performance, it is of great importance that the input parameters, including spatial distribution of aggregates, be highly tunable. The Sobolev packing algorithm was used to create a parametric aggregate dispersion for use in simulation of particulate composites (Figure 3.2a) [19-20].It was assumed that the aggregates had spherical shape (diameters varying from D_{min} to D_{max}) and that there was no contact between any two spheres within the predefined and controlled volume size. The packing size distribution and volumetric ratio of aggregates to matrix are highly tunable and parametric-based. This allows for future parameter coupling and output values for modeling real-scale particulate composites (Figure 3a).The packing algorithm starts with randomly assigning the location of the largest aggregate particle (D_{max}). The packing continues by the Monte-Carlo generation of the coordinates and subsequent placement of spheres with diameter d_i, wherein $D_{max} \geq d_i \geq D_{min}$. The center of the sphere must lie within the container and spheres must not overlap. Any spheres that do not fit these criteria are discarded.

After achieving a certain number of packing trials, the minimum sphere diameter, D_{min}, is reduced as follows:

where D_{min} is the minimum diameter, D_{max} is the maximum diameter, K is the reduction coefficient, and N is the number of trials.

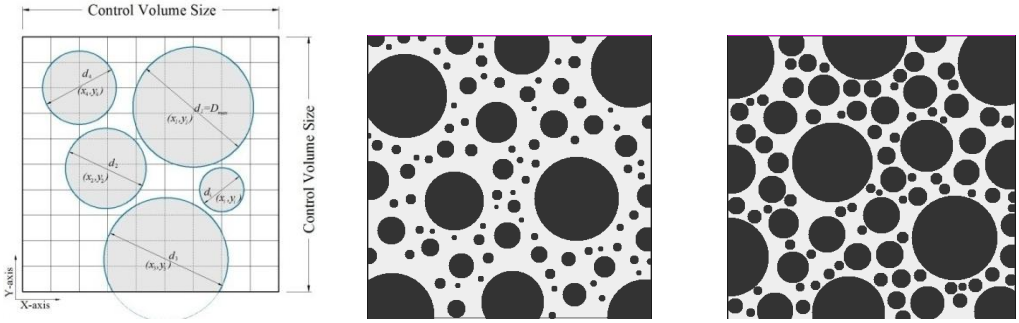

a) b) c)

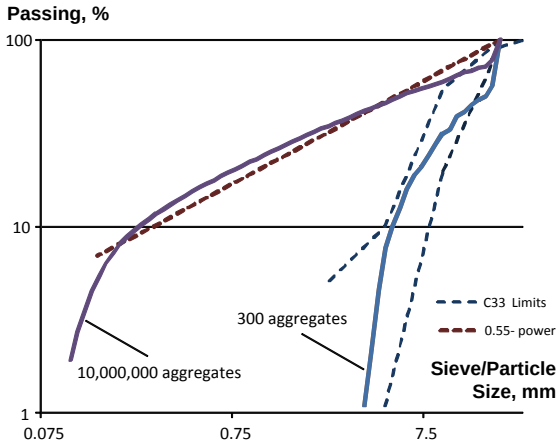

d)

Figure 3.2 The simulation based on Sobolev packing algorithm: (a) two-dimensional representation of the algorithm [19];the results of two-dimensional packing with (b) K= -1 and (c) K= -3 [7]; (d) particle size distribution for 3-dimensional packing of 300 and 10,000,000 aggregate particles.

This method yields a simple pseudo-dynamic packing algorithm that produces randomly packed set of aggregates in a given container [19-20].This method is further expanded to allow

coefficient-driven particle spacing, and, therefore, allowing a more realistic suspension model to be generated:

Where r is the radius of a new sphere, d is a minimum distance to the surface of any already packed set of spheres, k_{del} is an initial coefficient that provides the separation between spheres, S is a coefficient to change the size of separation, and m is the number of steps taken to change the size (for simplification, it is assumed that $m = N$).

This packing process yields a favorable result for the modeling of aggregate based composites when the spacing algorithm is applied, as demonstrated by Figure 2 [19-20]. It should be noted that the ultimate selection of the best aggregates. mix should be based on the workability requirements, segregation potential, strength and stiffness equirements achieved at the highest packing density possible [21]. Aggregate optimization can enhance the compressive strength by identification of the best blend through multiple criteria [22].

3.2 Finite Element Modeling

A finite element model of the cube shaped matrix containing spherical aggregates was created in ANSYS software. One set of generated 101 spheres were packed in an approximate cube shaped control volume . The spheres were scaled to have a maximum diameter of 20 mm. For the sake of simplicity, finer aggregates were not considered in the packing. A solid cube was then created in such a way that it accommodates all the spheres and at the same time it replicates a continuum of large scale pack . Outermost spheres were only partially contained inside the cube. The portion of those outermost spheres was then subtracted by boolean operation to flush the cut

surface of spheres to the outer surface of the cube. Another Boolean operation called glue was performed to tie the spheres to the cube so that they do not deform independently and freely under pressure.

The volumes were then meshed with ANSYS Solid65 concrete elements. Uniaxial pressure was applied to the block from the top surface while the bottom surface was constrained in all degrees of freedom. No slip condition of the top and bottom surfaces was considered. Material properties of the aggregate and mortar considered in this analysis are shown in Table 3.1

Table 3.1 Material properties of cement mortar and aggregates. [21]

	Elastic Modulus	**Poisson's Ratio**
Mortar/matrix	25 GPa	0.29
Aggregates	75 GPa	0.29

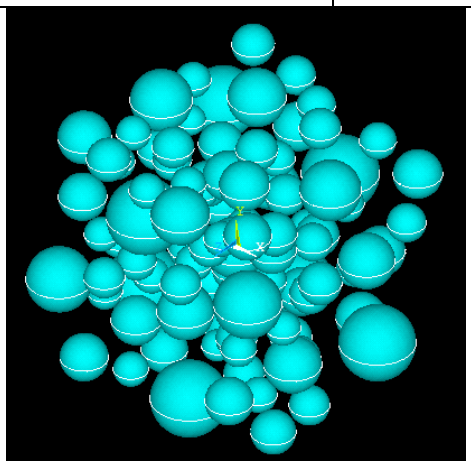

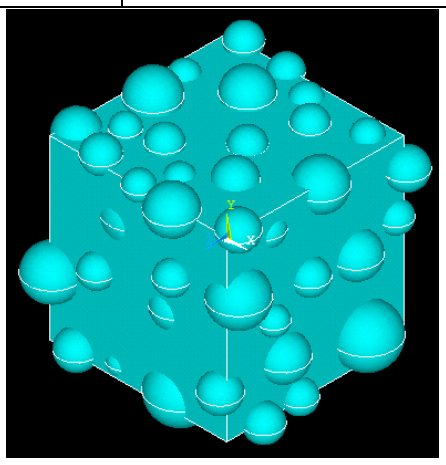

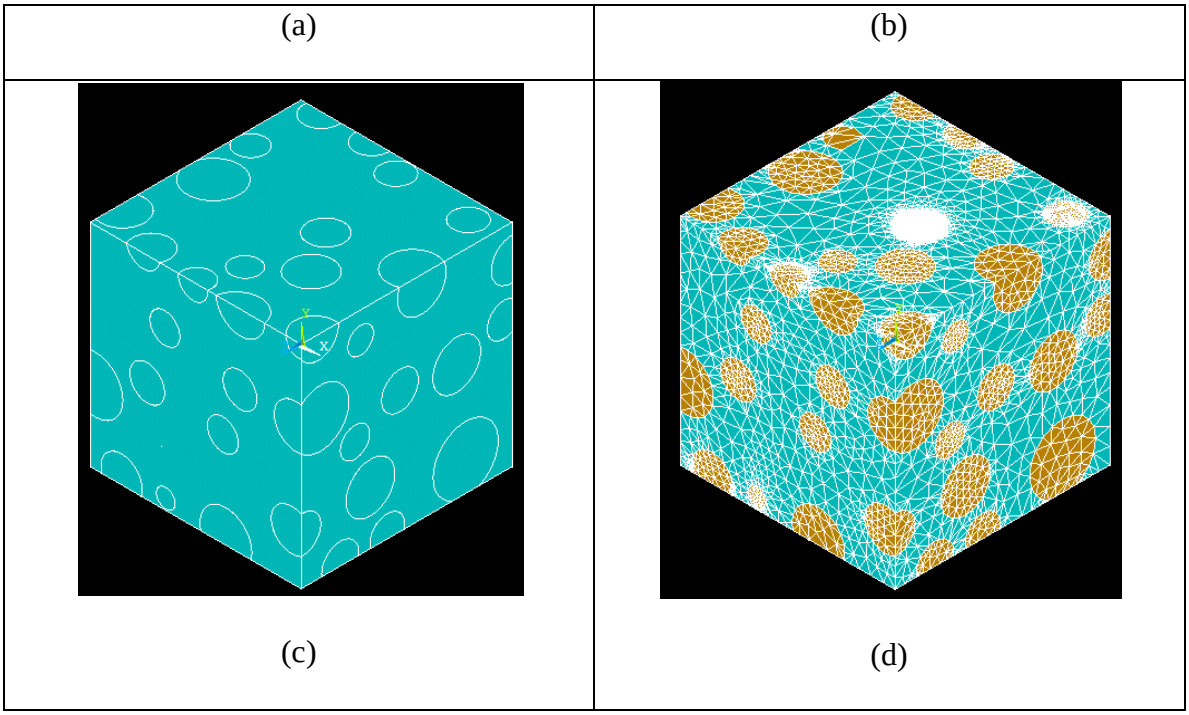

Figure 3.3: (a) Solid spheres generated in ANSYS from Sobolev packing algorithm, (b) solid block representing the RVE size (c) subtracting spheres outside the RVE (d) conformal finite element mesh.

3.2.1 SOLID65 3-D Solid Element

SOLID65 is used for the three-dimensional modeling of solids with or without reinforcing bars. The solid is capable of cracking in tension and crushing in compression. In concrete applications, for example, the solid capability of the element may be used to model the concrete while the rebar capability is available for modeling reinforcement behavior. Other cases for which the element is also applicable would be reinforced composites (such as fiberglass), and geological

materials (such as rock). The element is defined by eight nodes having three degrees of freedom at each node: translations in the nodal x, y, and z directions. Up to three different rebar specifications may be defined. The most important aspect of this element is the treatment of nonlinear material properties. The concrete is capable of cracking (in three orthogonal directions), crushing, plastic deformation, and creep.

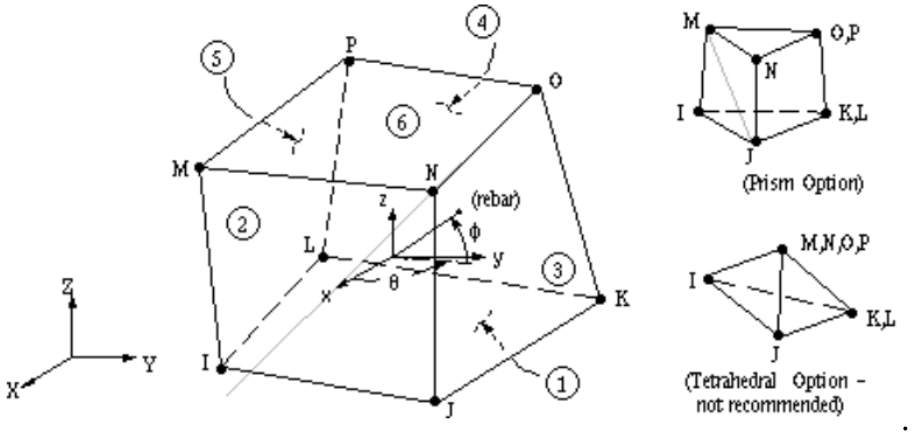

Figure 3-4 Node numbering convention and coordinate system of SOLID65 element.

CHAPTER 4

4 Results and Discussions

Since concrete, by construction, is a brittle material that does not exhibit a defined yield point. Moreover it has much lower strength is tension compared to the same in compression. So, in order to analyze the stresses, the maximum principal stresses were of primary concern. For comparison and boundary condition validation purposes the same boundary conditions were applied to a solid concrete block of the same size. By looking at the resulting stress contour plots it is found that the maximum stress zones resembles the actual laboratory test case. Figure 4.1, 4.2, 4.3 and 4.4 shows the 1^{st} principal stress, 2^{nd} principal stress, 3^{rd} principal stress and von Mises stress respectively for a solid concrete block.

In case of aggregate filled block the results of the stress contour are quite different from the results of an assumed homogeneous block. In the aggregate filled block the higher stress zones are located near and around the aggregates. Figure 4.5, 4.6, 4.7 and 4.8 shows the 1^{st} principal stress, 2^{nd} principal stress, 3^{rd} principal stress and von Mises stress respectively for aggregate filled concrete block.

From the results of stresses presented in Table 4.1 it is found that the stresses increase significantly with the inclusion of the aggregates.

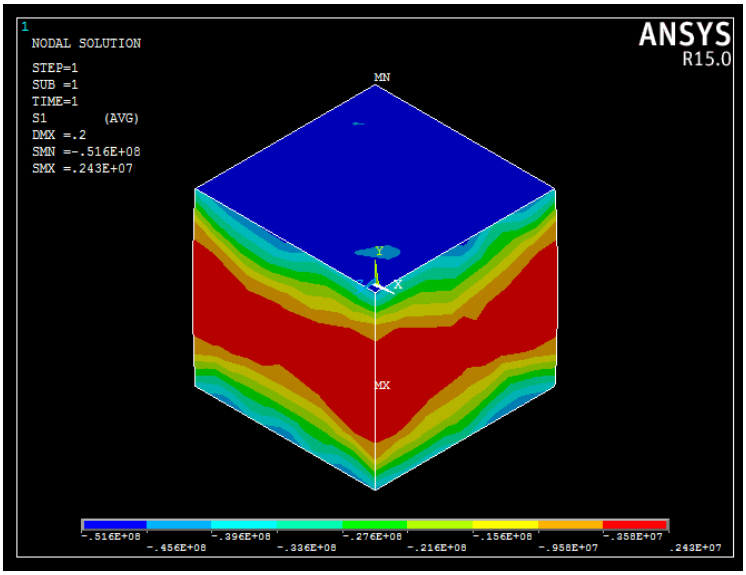

Figure 4-1 1st principal stress contour plot of solid concrete block.

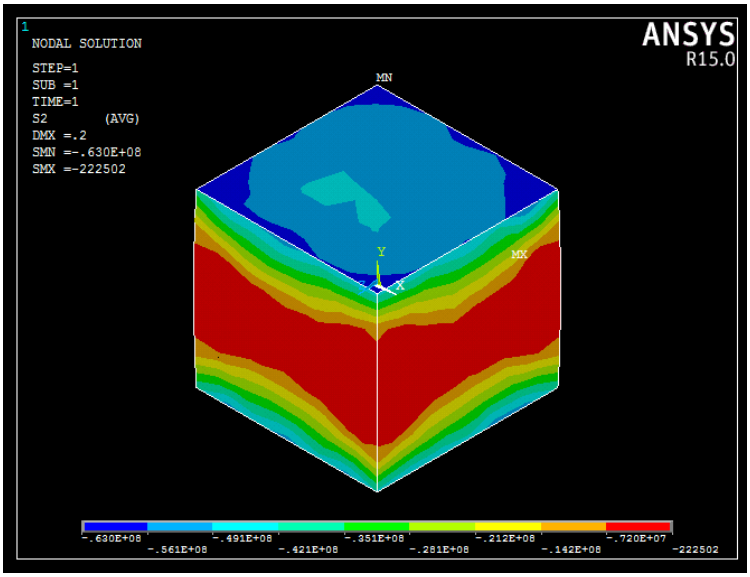

Figure 4.2 2nd principal stress contour plot of solid concrete block.

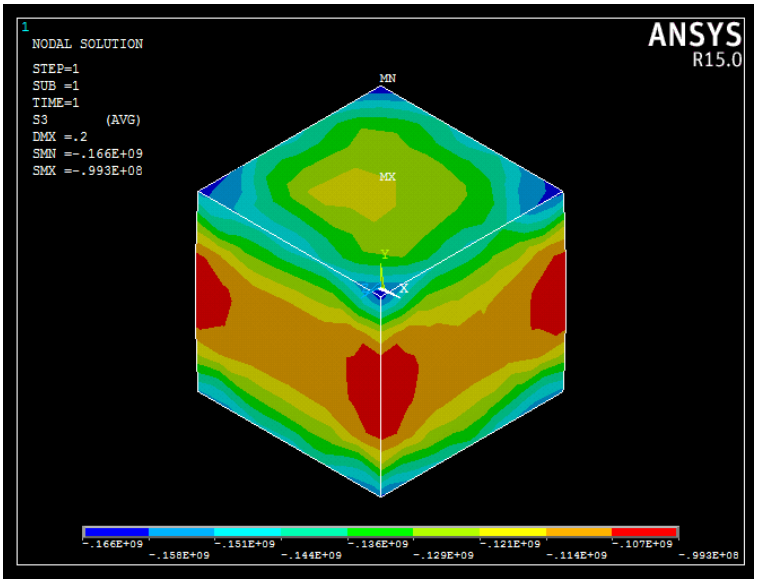

Figure 4.3 3rd principal stress contour plot of solid concrete block.

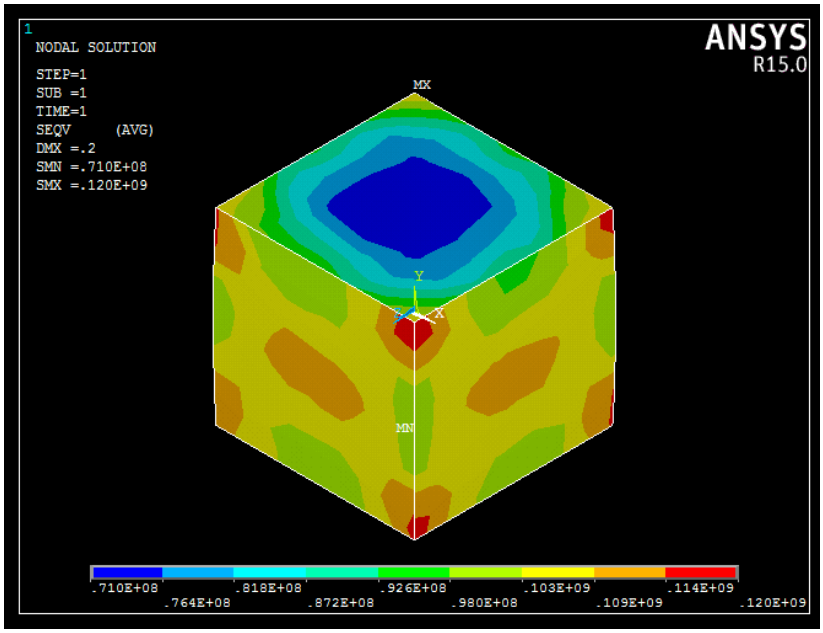

Figure 4.4 von Mises stress contour plot of solid concrete block.

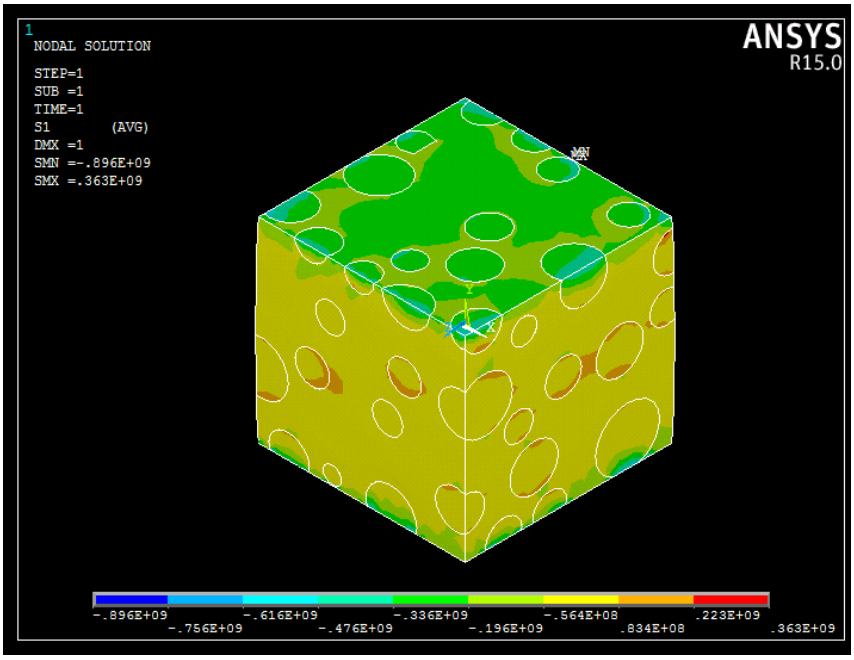

Figure 4.5 1st principal stress contour plot of aggregate packed concrete block.

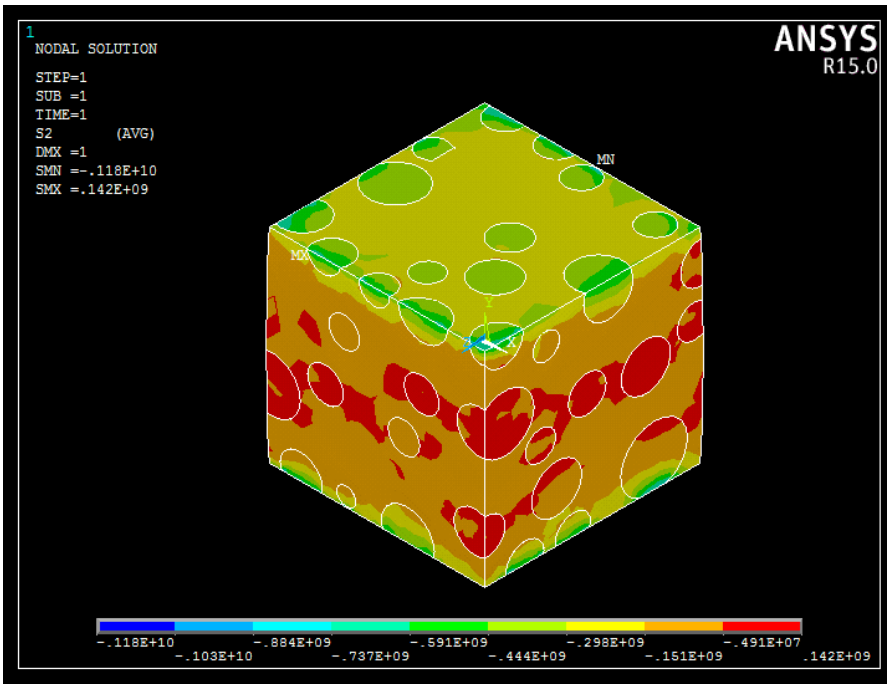

Figure 4.6 2nd principal stress contour plot of aggregate packed concrete block.

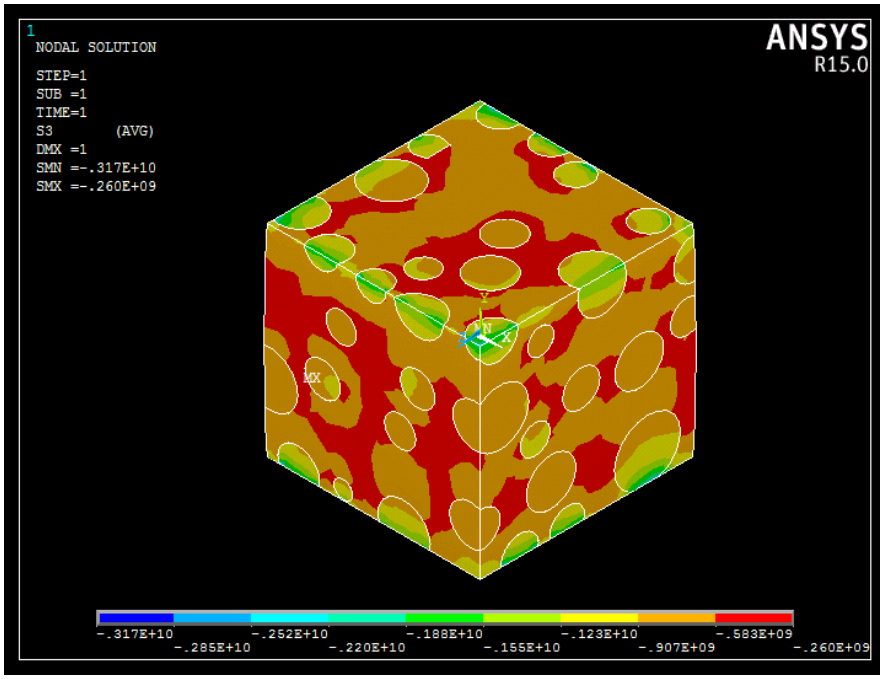

Figure 4.7 3rd principal stress contour plot of aggregate packed concrete block.

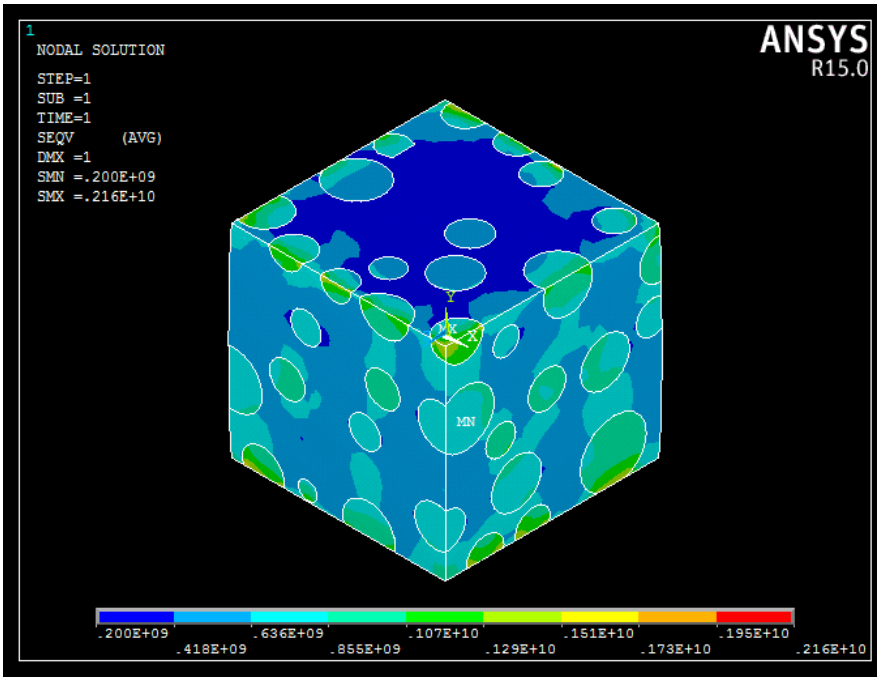

Figure 4.8 von Mises stress contour plot of aggregate packed concrete block.

Table 4-1 Stress result values for solid and aggregate filled concrete block.

	1st Principal Stress	**2nd Principal Stress**	**3rd Principal Stress**	**Von Mises Stress**
Solid Concrete Block	243 x 10^4 MPa	22 x 10^4 MPa	99 x 10^6 MPa	120 x 10^6 MPa
Aggregate Filled Concrete Block	363 x 10^6 MPa	142 x 10^6 MPa	260 x 10^6 MPa	216 x 10^7 MPa

CHAPTER 5

5 Conclusions and Future Work

Finite element models of solid concrete block and concrete block with aggregate packing were developed and analyzed for stresses. The constraints and loading conditions were validated through the solution of solid concrete block by looking at its maximum stress zones. Same boundary condition and loading were applied to the aggregate filled concrete block. As expected, the location and distribution of the maximum stresses were different from the same in the solid block. Results are summarized in the next sub-section..

5.1 Summary of Results

Results from the research are summarized below

- Finite element stress results for the solid concrete block replicates the actual test results of uniaxial compression on a concrete block. The higher stress zones are at the same location where the failure occurs.
- With inclusion of the aggregates the concrete block exhibits higher rigidity and consequently it experiences higher stresses.
- Higher stress occurs near the aggregates. It is because of the stress concentration at the aggregate-mortar interface. It indicates that damage or fracture is likely to initiate at the interface areas.
- 3-D solid-beam mixed element model shows lower stress than the solid only element model under same amount of bending (Figure 4-11).

5.2 Future Work

Several major research directions can be recommended for a future development of the finite element analysis of aggregate reinforced concrete:

1. Location of the crack initiation and nature of its propagation can be investigated through cohesive zone modeling in FEA.
2. Air voids were neglected throughout this research, where air voids play a significant role in concrete strength and fracture. Inclusion of air voids in the model will be a desired improvement of this research.
3. Investigating different types of loading conditions may be another approach to simulate different locations in a large structure.

REFERENCES

[1] Sobolev K, Amirjanov A. Application of genetic algorithm for modeling of dense packing of concrete aggregates. Const and Build Mater 2010;24(8):1449-1455.

[2] Sobolev K, Amirjanov A. A simulation model of the dense packing of particulate materials. Adv Powder Technol 2004;15: 365-376.

[3] Amirjanov A, Sobolev K. Fractal properties of Apollonian packing of spherical particles. Model Simul Mater Sci. Eng 2006; 14:789-798.

[4] Young J, Mindess S, Gray R, Benhur A. The Science and Technology of Civil Engineering Materials. U.S.: Prentice Hall, 1998. p.179-188.

[5] Hartsuijker C, Welleman JW. Engineering Mechanics Volume 2. U.S.: Springer, 2001.

[6] Ohama Y. Principle of Latex modification and some typical properties of Latex-modified mortar and concrete. ACI Mater Jour 1987; 84(6):511–518.

[7] Nagai G, Yamada T, Wada A. Finite Element Analysis of Concrete Material Based on The 3-dimensitioal Real Image Data, 4th World Congress on Computational Mechanics, Buenos Aires (1998).

[8] Li J, Liu Z , Qu X, Zhu C, Zhang Y. Finite element analysis of compressive strength of recycled coarse aggregate-filled concrete. Advanced Materials Research 2011;250-253,331.

[9] Leite J, Slowik V, Apel J. Computational model of mesoscopic structure of concrete for simulation of fracture processes. Computers & Structures 2007;85(17/18):1293-1303.

[10] He H, Stroeven P, Stroeven M, Sluys L. Influence of particle packing on elastic properties of concrete. Magazine of Concrete Research 2011;64(2):163-175

[11] Elias J, Stang H. Lattice modeling of aggregate interlocking in concrete. International Journal of Fracture 2012;175(1):1-11.

[12] Gal E, Kryvoruk R. Meso-scale analysis of FRC using a two-step homogenization approach. Computers & Structures 2011;89(11/12),921-929.

[13] Wriggers P, Moftah S. Mesoscale models for concrete: Homogenisation and damage behaviour. Finite Elements in Analysis & Design 2006;42(7),623-636.

[14] Kasai A. Multiscale modeling and simulation of concrete and its constituent materials. (Doctoral thesis) 2008. University of Mississipi: USA.

[15] Chaudhuri, P. (2013). Multi-scale modeling of fracture in concrete composites. Composites Part B: Engineering, 47, 162-172.

[16] M.Y.H.Bangash. Concrete and Concrete structures: Numerical Modelling and Applications. London : Elsevie Science Publishers Ltd., 1989

[17] D. Cioranescu and P. Donato. An introduction to homogenization. Oxford University Press, 1999.

[18] O. Lloberas-Valls, D.J. Rixen, A. Simone, and L.J. Sluys. Domain decomposition techniques for the ecient modeling of brittle hetero- geneous materials. Computer Methods in Applied Mechanics and Engineering, 200(13-16):1577{1590, 2011.

[19] SobolevK,Amirjanov A. Application of genetic algorithm for modeling of dense packing of concrete aggregates. Const and Build Mater 2010;24(8):1449-1455.

[20] SobolevK,Amirjanov A. A simulation model of the dense packing of particulate materials.Adv Powder Technol 2004;15: 365-376.

[21] Moini, Mohamadreza, "The Optimization of Concrete Mixtures for Use in Highway Applications." (2015).

[22] Moini Mohamadreza, Muzenski Scott, Ismael Flores-Vivian, Sobolev Konstantin "Aggregate optimization for concrete mixtures with low cement factor", 3rd All-Russia (2nd International) Conference on Concrete and Reinforced Concrete: Glace at Future, Vol. 4, Moscow, May 12, 2014, pp. 349–59.

[23] Moini M., Flores-Vivian I., Amirjanov A., Sobolev K., The Optimization of Aggregate Blends for Sustainable Low Cement Concrete. Construction & Building Materials Journal, 2015.

[24] Konstantin Sobolev, Mohamadreza Moini, Steve Cramer, Ismael Flores-Vivian, Scott Muzenski, Rani Pradoto, Ahmed Fahim, Le Pham, Marina Kozhukhova, “Laboratory Study of Optimized Concrete Pavement Mixtures”, WHRP 0092-13-04.